actuators

MDPI

Article

Programmable Hydrogel-Based Soft Robotics via Encoded Building Block Design

Sirawit Pruksawan [1], Zhan Au Chua [1,2], Yi Ting Chong [1] and FuKe Wang [1,*]

[1] Institute of Materials Research and Engineering (IMRE), Agency for Science, Technology, and Research (A*STAR), 2 Fusionopolis Way, Innovis #08-03, Singapore 138634, Singapore; sirawit_pruksawan@imre.a-star.edu.sg (S.P.); chongyt@imre.a-star.edu.sg (Y.T.C.)

[2] College of Design and Engineering, National University of Singapore (NUS), 4 Engineering Drive 3, Singapore 117585, Singapore

* Correspondence: wangf@imre.a-star.edu.sg

Abstract: Hydrogels have revolutionized the field of soft robotics with their ability to provide dynamic and programmable responses to different stimuli, enabling the fabrication of highly adaptable and flexible robots. This continual development holds significant promise for applications in biomedical devices, active implants, and sensors due to the biocompatibility of hydrogels. Actuation in hydrogel-based soft robotics relies on variations in material properties, structural design, or a combination of both to generate desired movements and behaviors. While such traditional approaches enable hydrogel actuation, they often rely on complex material design, bringing challenges to hydrogel fabrication and hindering practical use. Therefore, this work seeks to present a simplified and versatile approach for fabricating programmable single-component hydrogel-based soft robotics using an encoded building block design concept and 3D printing. A series of structural building blocks have been designed to achieve various actuation characteristics, including the direction, degree, and kinetics of actuation. By assembling these building blocks into various configurations, a broader range of actuation responses can be encoded, allowing for the fabrication of versatile, programmable soft robotics using a single uniform material through vat photopolymerization 3D printing. This approach enables adaptation to a wide range of applications, providing highly customizable encoding designs.

Keywords: hydrogel; soft robotics; 3D printing; actuation; material coding

check for updates

Citation: Pruksawan, S.; Chua, Z.A.; Chong, Y.T.; Wang, F. Programmable Hydrogel-Based Soft Robotics via Encoded Building Block Design. *Actuators* **2024**, *13*, 383. https://doi.org/10.3390/act13100383

Academic Editors: Amir Jafari and Trevor Exley

Received: 2 September 2024
Revised: 20 September 2024
Accepted: 25 September 2024
Published: 1 October 2024

Copyright: © 2024 by the authors. Licensee MDPI, Basel, Switzerland. This article is an open access article distributed under the terms and conditions of the Creative Commons Attribution (CC BY) license (https://creativecommons.org/licenses/by/4.0/).

1. Introduction

Recently, hydrogels have emerged as a promising candidate for soft actuators, offering unique properties such as high adaptability, broad responsiveness, and biocompatibility [1–3]. These capabilities are crucial for advancing soft robotics and other cutting-edge applications, particularly in the biomedical field [4–6]. By mimicking the natural flexibility and adaptability of biological tissues, hydrogel-based actuators enable soft robots to perform complex tasks in dynamic environments, making them ideal for advanced bio-applications such as soft surgical robots, soft sensors, soft grippers, and drug delivery systems [7–10]. Current hydrogel-based actuators primarily rely on variations in material properties within the actuator to induce actuation. Gradients in swelling, thermal, and light responses, among others, are achieved through variations in material properties [11,12], the combination of multiple materials [13–15], or the addition of functional fillers [16,17], enabling controlled and precise movements. Although these approaches have proven effective in achieving diverse actuation responses to different environmental stimuli, they have introduced several complexities and fabrication challenges that can limit their practical applicability. Specifically, incorporating gradients can lead to inconsistencies in properties such as mechanical stress across the material [12], potentially compromising its practical performance and usability. Additionally, the fabrication processes required to create these gradients—such as layer-by-layer deposition [11], multi-stage mold casting [15], and

multi-material printing [13]—can be specialized and may limit the design possibilities for hydrogel-based actuators.

Given the complexities associated with gradient-based approaches for inducing actuation, we recently developed a simpler and effective solution by achieving hydrogel-based actuation through gradient swelling kinetics, focusing on design rather than material component tuning [18]. This work demonstrates the feasibility of printing hydrogel structures on a common DLP printer with a uniform single-material composition, while inducing actuation via controlled gradient swelling kinetics. This approach simplifies fabrication by requiring only design modifications, allowing the use of single-component hydrogels in most vat photopolymerization-based printing systems. However, systematic control of the actuation, along with programmable actuation changes, remains unclear. For practical applications, a deeper understanding of the actuation response—including direction, degree, and kinetics—is necessary. Further investigation is required to expand the design possibilities and enable the creation of actuators that are highly programmable, controllable, and customizable for efficient use in practical applications.

In this work, we present a simplified and versatile approach for fabricating programmable single-component hydrogel-based soft robotics by leveraging an encoded building block design concept and 3D printing. Rather than relying on the intrinsic stimuli-responsive properties of hydrogels—such as response to electricity, light, heat, or pH—to induce actuation, we achieved a range of actuation responses through the strategic design of 3D-printed hydrogel structures. This approach uses a single material with specifically designed structures to generate gradient swelling, as opposed to previous works that utilized non-uniform materials with gradient crosslinking, fillers, or compositions [11–17,19]. The use of a single material ensures uniform properties, enhancing the consistency and reliability of mechanical and thermal performance for practical applications. Furthermore, we introduced a strategic design framework that facilitates the development of more complex hydrogel-based soft robotics through customized encoding designs, allowing for a broader range of actuation responses compared to the limited programmability of actuations in our previous work [18]. By focusing on design, we create various building block units with diverse actuation movements and kinetics, enabled by gradient swelling through systematically designed diffusion-path architectures. These building blocks are encoded into versatile structures to generate different hydrogel-based actuators with high programmability. Due to the simplicity of direct fabrication and the versatility of material choice, this approach streamlines the material design process and facilitates easy adaptation to diverse applications with customized encoding designs. In Section 3.1, we optimize the programmability of actuators by testing different hydrogel precursor compositions to achieve the highest actuation performance. Section 3.2 details the design and utilization of various building block units with different designs for actuation. The optimal building block is then selected and extended as repeated units to enhance programmability, achieving various controllable responses and kinetics in actuators. Section 3.3 demonstrates the reversibility and equilibrium of the hydrogel actuators using this concept. In Section 3.4, we assemble the designed building blocks into different configurations to achieve various actuation responses in soft robotics, referred to as the encoded building block design. Finally, Section 3.5 showcases the potential application of hydrogel soft robotics as a manipulator for transporting objects from one position to another. All these aspects demonstrate the simplicity of adaptation, high programmability, versatility, and practical applications of the approach.

2. Experimental Section

2.1. Materials

Acrylic acid (AC) (99% purity), acrylamide (AM) (99% purity), triethylene glycol dimethacrylate (TEGDMA) (95% purity), and rhodamine B were obtained from Sigma-Aldrich (Singapore) and used without further purification. Lithium phenyl-2,4,6-

trimethylbenzoylphosphinate (LAP) was provided by TCI Chemical (Singapore) and used without further purification.

2.2. Preparation and 3D Printing of Hydrogels

The hydrogel precursor was prepared as follows: 60 g of acrylamide and acrylic acid monomer with specific ratios (60:0, 45:15, 30:30, 15:45, 0:60) was dissolved in 38 g of deionized water and sonicated for approximately 20 min until fully dispersed. TEGDMA (1.5 g) was added as a crosslinker, LAP (0.5 g) as a photoinitiator, and rhodamine B (0.025 g) as a photo-absorber. The mixture was further sonicated to ensure complete dissolution, resulting in a hydrogel precursor for subsequent 3D printing.

The prepared hydrogel precursor was then 3D printed using an Anycubic Photon Mono 4K printer equipped with a liquid crystal display (LCD) shadow masking technique (Shenzhen Anycubic Technology Co., Ltd., Shenzhen, China). 3D models were designed and generated using Autodesk Fusion 360 software (v.2.0.19941), exported in Stereolithography (STL) format, and imported into the Anycubic Photon Workshop 3D Slicer software for slicing. Each printing layer was set to a thickness of 0.05 mm, with a light intensity of 70%, and an exposure time of 7.4 s per layer. No bottom layers were used. Once the slicing file was imported, the hydrogel precursor was poured into the printer's vat, and the printing process commenced layer by layer. After printing, the hydrogel samples underwent post-curing in a UV oven using Anycubic Wash and Cure 3.0 (Shenzhen Anycubic Technology Co., Ltd., China) and were stored in a refrigerator at 4 °C before further testing and characterization. All 3D-printed samples were characterized to achieve a printing accuracy up to 0.15 mm, fulfilling the feature that appeared in the STL design model.

2.3. Material Testing and Characterization

Tensile testing of the hydrogels was conducted using an Instron 5569 double-column universal testing machine (Instron, Norwood, MA, USA) equipped with a 100 N load cell, following ASTM D638 standards adapted for hydrogel materials [20,21]. Hydrogel samples, sized 10 mm × 60 mm × 1.6 mm, were securely held using pneumatic grips and marked at two vertical positions for tensile strain detection. An extensometer precisely determined tensile strain based on these marked points. The specimens were elongated at a strain rate of 40 mm per minute until fracture, with a minimum of three samples tested under each condition. The tensile strength of the hydrogels was calculated by dividing the maximum load by the original cross-sectional area of the test specimen.

Swelling tests were conducted on as-prepared hydrogel samples with various design models under different pH conditions and over varying time intervals. Initially, the hydrogel samples were weighed to obtain their initial weight (W_i). Subsequently, the samples were immersed in deionized water for predetermined periods. At specific time points, the samples were removed, excess surface water was gently removed using tissue paper, and the samples were reweighed to obtain the swollen weight (W_t). Triplicate samples were taken, and the average values were reported along with the standard deviation. The swelling ratio was determined using the following formula [22]:

$$Swelling\ ratio\ (\%) = \frac{W_t - W_i}{W_i} \times 100$$

A hydrogel curling test was conducted to evaluate the degree of curling across various hydrogel formulations and design models. Initially, samples were meticulously placed in containers to ensure that no pre-existing curl or dimensional deviations from the original design were present. Upon initiation of the test, a specific solution was introduced, and images were captured at designated time intervals. The end-to-end distance of each sample was quantified using ImageJ software (National Institute of Health (NIH), MA, USA). Each test was performed in triplicate, with results presented as average values and standard deviations to accurately represent the degree of curling for each condition.

3. Results and Discussion

3.1. Material Composition and Programmability of Hydrogels

This section explores the effect of material composition on the programmability of hydrogels before addressing design aspects in the following sections. The hydrogels studied are made from blends of acrylamide (AM) and acrylic acid (AC) in the ratios 60:0, 45:15, 30:30, 15:45, and 0:60, with triethylene glycol dimethacrylate (TEGDMA) used as a crosslinker to adjust both mechanical properties and programmability (see Section 2.2 for detailed composition). The mechanical properties are critical to an actuator's performance, as they govern the material's movement and deformation in response to applied forces [2,23]. Figure 1A shows that hydrogels with a higher acrylamide content compared to an equivalent mixture (i.e., AM:AC = 45:15, 60:0) exhibit significantly lower mechanical performance in terms of tensile strength and fracture strain. This occurs because acrylamide forms a more flexible polymer network with a less densely crosslinked structure [24]. In contrast, the carboxyl groups in acrylic acid form ionic bonds, creating a more rigid and tightly crosslinked network [25,26]. Hydrogels with lower acrylamide content (AM:AC = 0:60, 15:45, 30:30) demonstrate considerably stronger mechanical properties, with tensile strengths exceeding 1 MPa and fracture strains above 500%. The optimal mechanical performance is observed at the equal ratio of acrylamide to acrylic acid (AM:AC = 30:30), likely due to the balanced interplay between the flexibility of acrylamide and the rigidity of acrylic acid.

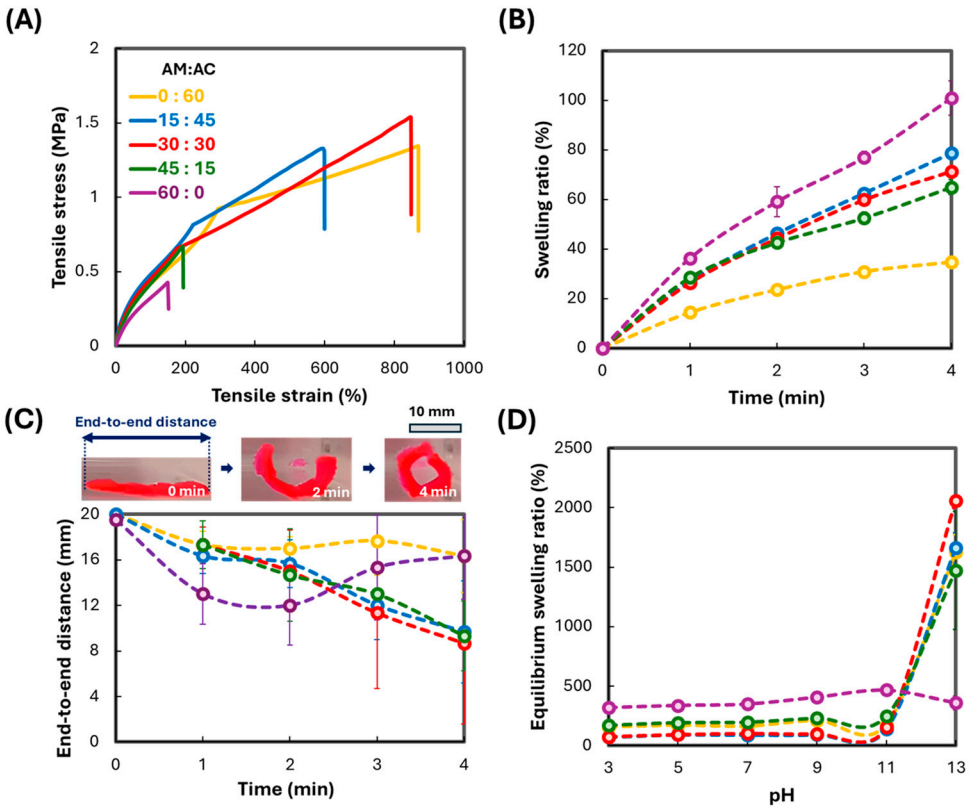


Figure 1. Effect of Material Composition on Hydrogel Properties and Programmability. (**A**) Tensile stress–strain curves of hydrogels. (**B**) Swelling ratio of hydrogels after initial immersion in pH 13 solution for 4 min. (**C**) End-to-end distance of hydrogels following exposure to pH 13 solution for 4 min. The inset shows the curling of a hydrogel with an AM/AC ratio of 30:30 and the corresponding measurement of the end-to-end distance. (**D**) Equilibrium swelling ratio of hydrogels in solutions of varying pH. The acrylamide-to-acrylic acid ratios (AM:AC) are 0:60, 15:45, 30:30, 45:15, and 60:0, represented by different line colors as defined in (**A**). Error bars indicate standard deviations.

The swelling characteristics of these hydrogels in pH 13 solution during the initial swelling phase were examined (Figure 1B). The swelling kinetics provide insights into the

water absorption rate of each hydrogel and their internal network structure in relation to their actuation behavior during the initial swelling. The hydrogel composed of pure acrylamide (AM:AC = 60:0) exhibited the highest swelling, reaching 100.8% within 4 min, due to the flexibility of the polyacrylamide network. In contrast, the hydrogel made with pure acrylic acid (AM:AC = 0:60) showed the lowest swelling, reaching only 34.6% within the same period, owing to its high rigidity. This indicates that, in our study, polyacrylamide swells more readily compared to polyacrylic acid, suggesting a looser morphological structure for polyacrylamide. Hydrogels with blended acrylamide and acrylic acid (AM = 15:45, 30:30, 45:15) displayed moderate swelling ratios, with values falling between those of the pure components.

These hydrogels were further tested for actuation upon initial swelling in pH 13 solution by being 3D printed in the Model D(4) shape (Figure 1C). The printed hydrogels were activated by soaking in water, which induced curling. Although actuation is driven by water absorption and can occur at any pH level, pH 13 was selected because it accelerates the response of polyacrylic acid, potentially enhancing the degree of swelling and, consequently, the extent of actuation. The actuation of the hydrogel is facilitated by shape transformation through gradient swelling within its sloped and narrowed structure, influenced by the printed design. The hydrogel structure is printed with varying surface area-to-volume ratios across different regions to achieve gradient swelling. This gradient induces a non-uniform stress distribution, leading to shape transformation upon swelling [18,19]. Regions with higher stress deform more prominently due to differential expansion, creating an imbalance in stresses that drives the transformation of the overall structure. The actuation was quantified by measuring the end-to-end distance of the specimen (photos to be inserted in Figure 1C). Since the curling angle may vary along the length of the structure due to structural asymmetry, this end-to-end distance is used to represent the overall degree of curling and reflects the actuation level of the hydrogel. Notably, the hydrogel with an equal mixture of acrylamide and acrylic acid (AM:AC = 30:30) exhibited the largest change in end-to-end distance, reducing from 20 mm to 9 mm within 4 min, demonstrating a significant actuation effect. The hydrogel with pure acrylic acid showed minimal actuation, while the hydrogel with pure acrylamide displayed good initial actuation during the first minute after soaking but no further curling, likely due to its softness and therefore inability to support the entire structure. These results suggest that the hydrogel with AM:AC = 30:30 is the most optimal for actuation applications, offering a balanced combination of flexibility and rigidity. Hydrogels with high rigidity are too stiff to curl effectively, while those with high softness lack the structural integrity needed for sustained actuation.

The equilibrium swelling ratios of all hydrogels were characterized at various pH levels to investigate their swelling and pH responsiveness beyond the initial swelling. The pure polyacrylamide hydrogel (AM:AC = 60:0) showed nearly the same equilibrium swelling ratio across all measured pH levels ranging from 3 to 13, due to the lack of pH-responsive properties in polyacrylamide. In contrast, hydrogels containing acrylic acid (AM:AC = 15:45, 30:30, 45:15, 60:0) exhibited pH responsiveness [27,28], with a significant increase in equilibrium swelling ratio at pH 13, reaching up to 2059% swelling in the AM:AC = 30:30 sample. Considering its effective actuation, balanced mechanical properties, and responsive pH behavior, the AM:AC ratio of 30:30 is selected as the hydrogel formulation for further actuation development, with a focus on design optimization.

3.2. Design of Building Block Units

Two sets of designs were developed: (A) geometric building block units and (B) building block assemblies (Figure 2). For the geometric building block unit, a simple rectangular unit with dimensions of 20 cm in length and 1.5 cm in height was used as the control geometry, designated as Model A. In Model B, C and D, a different approach to generate swelling gradients within the structures introduced the utilization of different geometry designs with controlled structure surface area and volume across the models. These gradients

induce a non-uniform stress distribution, leading to deformation and shape transformation within the structure. In Model B, a height gradient was introduced to generate a swelling gradient along the height (Z-direction) while maintaining the same volume, surface area, and unit length. Similarly, Model C incorporated a width gradient across the X direction while keeping the volume, surface area, and maximum height constant. Model D combined both height and width gradients to maximize the swelling gradient within the unit while maintaining the same volume and surface area as the other models. As shown in Table 1, Models A, B, C, and D have the same volume and surface area, with the unit length kept consistent to ensure a fair comparison. In the building block assembly, Model D was used as the building block unit. This unit was assembled in single, double, triple, and quadruple configurations, denoted as Models D(1), D(2), D(3), and D(4), respectively. This approach is anticipated to enhance the swelling gradient of the hydrogel samples, as indicated by the increased surface-area-to-volume ratio shown in Table 1, from 1.57 in Model D(1) to 1.62, 1.69, and 1.76 in Models D(2), D(3), and D(4), respectively.

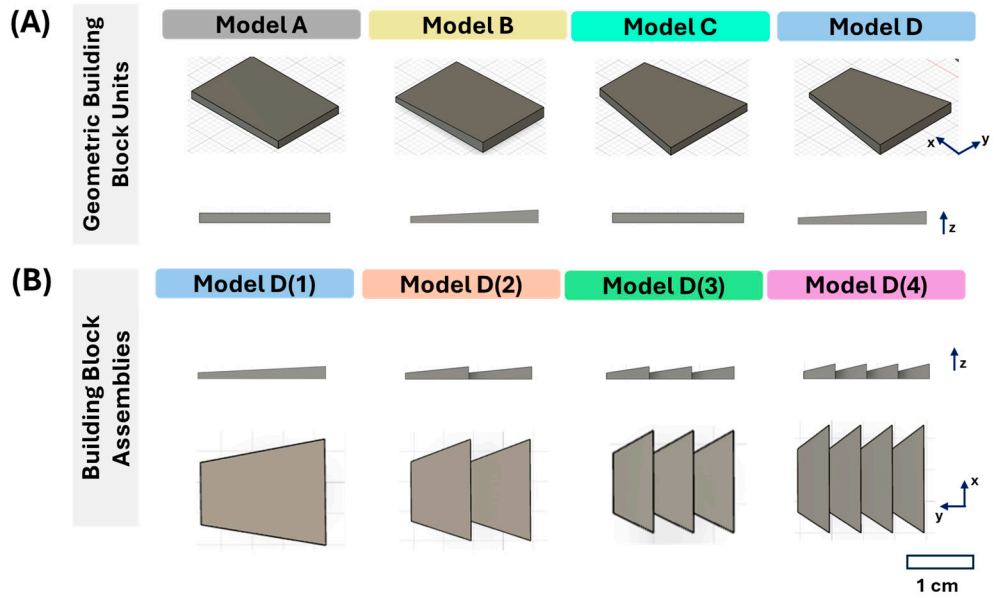


Figure 2. Design of 3D Model for Hydrogel Printing. (**A**) Geometric configuration designs: Models A, B, C, and D. (**B**) Modular assembly designs: Models D(1), D(2), D(3), and D(4). Scale bar: 1 cm.

Table 1. Design Specifications of 3D models Used for Hydrogel Printing.

STL Model	A	B	C	D/D(1)	D(2)	D(3)	D(4)
Volume (cm^3)	4.2	4.2	4.2	4.2	4.2	4.2	4.2
Surface area (cm^2)	6.6	6.6	6.6	6.6	6.8	7.1	7.4
Surface-area-to-volume ratio	1.57	1.57	1.57	1.57	1.62	1.69	1.76
Unit length (mm)	20	20	20	20	20	20	20

Hydrogels printed with different building block unit models (A, B, C, and D) were subjected to actuation tests upon soaking in pH 13 solution (Figure 3). Hydrogels with Models A and C exhibited minimal curling, while those with Models B and D showed more pronounced curling (Figure 3A). This curling was quantitatively assessed by measuring the end-to-end distance of the specimens (Figure 3B). Model A displayed almost no change in end-to-end distance due to its symmetric design, while Model C showed minimal change, likely due to the limited swelling gradient induced by the width variation. The height gradient appears effective in inducing actuation, as evidenced by Model B's clear reduction in end-to-end distance after soaking. However, Model D exhibited the most significant

reduction in end-to-end distance, as it effectively combines gradients in both the Z and XY directions to enhance the curling effect, aligning with our expectations.

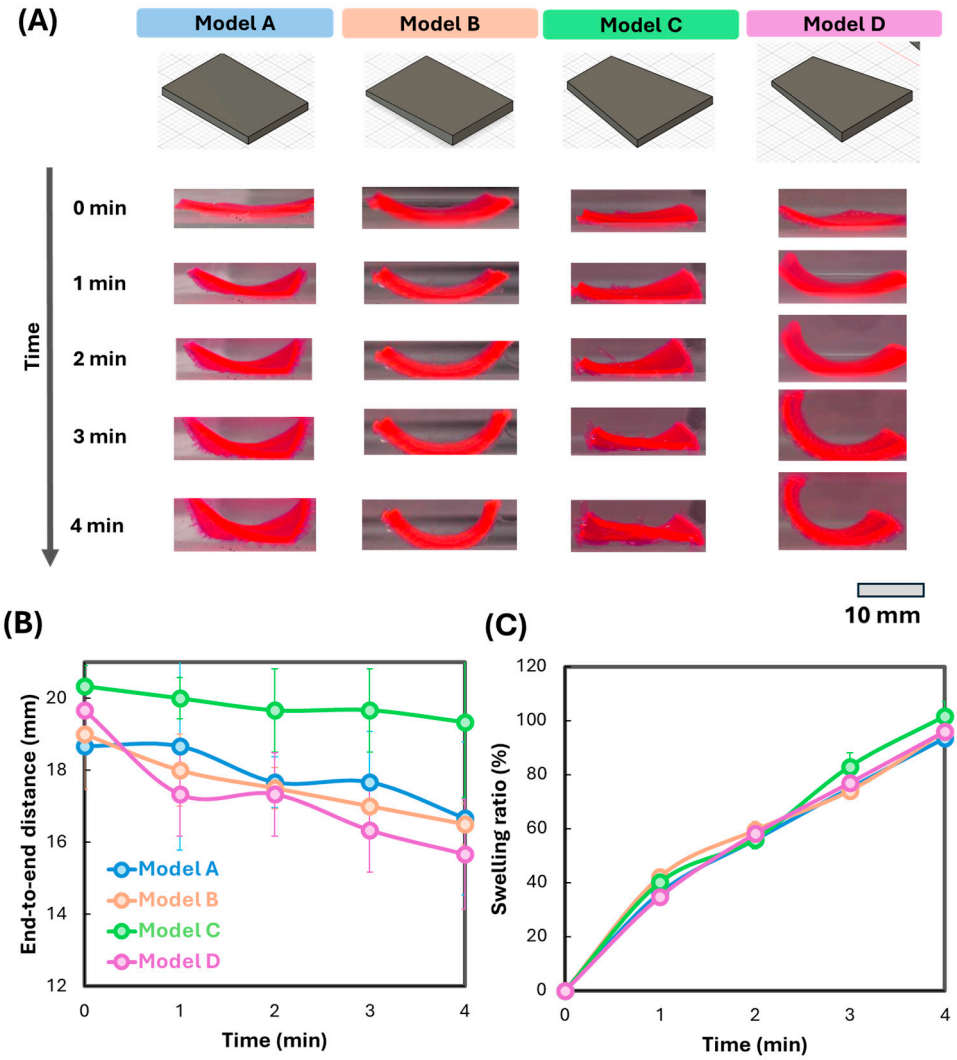


Figure 3. Hydrogel Soft Robotics with Different Building Block Unit Designs in pH 13 solution. (**A**) Curling behavior of the hydrogel during swelling over 4 min. (**B**) End-to-end distance of the curling hydrogel during swelling over 4 min. (**C**) Swelling ratio of the hydrogel during swelling over 4 min. Error bars indicate standard deviations.

The swelling ratios during the 4-min actuation for Models A, B, C, and D are shown in Figure 3C. All specimens swell to a similar degree and at a similar rate with no significant differences observed. Therefore, a more rigorous approach was employed, involving the analysis of the swelling behavior of each section within the model. This method yielded substantial difference. The swelling ratios of the left and right sections of the specimens were measured separately after cutting them into two parts of equal length and performing swelling tests in water. The results are summarized in Table 2. This investigation was conducted to understand the swelling response in each section of the model, which contributes synergistically to inducing actuation. Models A, B, and C exhibited smaller differences in swelling ratios between the sections (<10%), while Model D demonstrated a larger difference of up to 24.4% after 4 min. This variation in swelling ratios within the unit leads to actuation, specifically curling of the hydrogel, due to non-uniform swelling. Therefore, Model D is suitable for use as an actuation building block unit, as it is designed to have significant swelling gradients within the unit. This model will be utilized in the next

stage of design. Furthermore, this demonstrates that the actuation response of hydrogels can be effectively achieved through the strategic design of 3D-printed hydrogel structures at a fixed pH.

Table 2. Swelling Ratios of Hydrogels Printed with Different 3D Models and Sectioned to Determine Swelling Ratio Differences.

Swelling Ratio at 4 min (%)	A	B	C	D
Left section	123.1	81.5	132.6	100.7
Right section	115.3	75.8	140.7	75.9
Difference (Left − Right)	7.8	5.8	8.0	24.8

Model D was used as the building block unit and further assembled into single, double, triple, and quadruple configurations to demonstrate the programmability of the actuator. The number of assembled building block units resulted in different curling responses, with the specific outcomes in pH 13 solution shown in Figure 4A and Video S1. At this pH, the actuator demonstrates a faster response mode compared to lower pH levels, where a slower response occurs. The hydrogel with Model D(1) exhibited the least degree of curling, while Models D(2), D(3), and D(4) showed progressively greater curling responses, corresponding to the increasing number of assembled building block units. Not only did the degree of curling increase, but the timing of the curling response also varied with the number of units. The end-to-end distance of specimens over time characterized these curling kinetics (Figure 4B). The hydrogel with Model D(4) began curling within a few seconds of soaking, whereas Models D(1), D(2), and D(3) showed delayed curling after several minutes. These results suggest that assembling multiple building block units significantly enhances the programmability of the actuator. The curling behavior of individual units contributes to an increased degree of curling and a faster curling rate as the number of units is expanded. Additionally, Figure 4C shows that the swelling rate of Model D(4) is significantly larger than that of the other models, likely due to its higher surface area-to-volume ratio, as shown in Table 1. Model D(4) has a surface area-to-volume ratio of 1.76 compared to 1.57, 1.62, and 1.69 for Models D(1), D(2), and D(3), respectively. This larger surface area facilitates water diffusion during the initial swelling, increasing the swelling rate and thereby contributing to a larger swelling gradient. These findings highlight the potential for designing a wide range of programmable actuators with responses that vary from slow to fast and from low to high degrees of actuation, tailored to specific practical applications. This advancement holds significant potential for developing versatile actuators with enhanced programmability.

While the actuation of the hydrogels is predominantly governed by the 3D design, pH also plays a crucial role in their performance. As polyacrylic acid-based hydrogels, these materials exhibit pH-responsive behavior, leading to faster and more pronounced swelling at higher pH levels [27,29], as detailed in Section 3.1. The performance of hydrogel actuators with varying numbers of building block units is demonstrated at pH 7 in Figure 5, in comparison to pH 13 shown in Figure 4. The response at pH 7 is noticeably less pronounced than at pH 13; however, curling still occurs, even though to a lesser degree. During initial 4 min soaking in pH 7 solution, all actuators exhibit slow and relatively uniform curling (Figure 5A), with the end-to-end distance gradually reducing from approximately 20 mm to around 18 mm for all specimens. Additionally, the swelling kinetics of all specimens display similar trends, as illustrated in Figure 5C. These results indicate that pH can significantly influence the actuation process, complementing the effects of the encoding building block design and enhancing the programmability of the actuators. This adaptability allows for modifications in response based on changes in stimuli, such as pH, temperature, ionic strength, or UV light [27,30,31]. Thus, the combination of our encoding building block design with traditional responsive hydrogels demonstrates a highly versatile and programmable actuator suitable for advanced applications. The results also show that actuation occurs at a lower pH, although the response is delayed compared to a higher pH, which can be advantageous in avoiding the use of high pH in certain undesired situations.

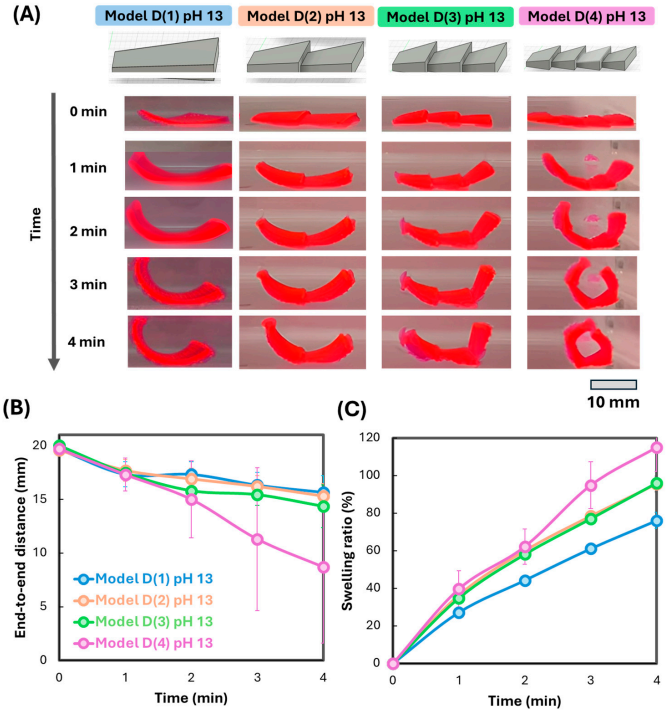


Figure 4. Hydrogel Actuators with Varying Numbers of Building Block Units at pH 13. (**A**) Curling behavior of the hydrogel during swelling over 4 min. The video of the hydrogel curling can be found in Video S1 of the Supplementary Materials. (**B**) End-to-end distance of the curling hydrogel during swelling over 4 min. (**C**) Swelling ratio of the hydrogel during swelling over 4 min. Error bars indicate standard deviations.

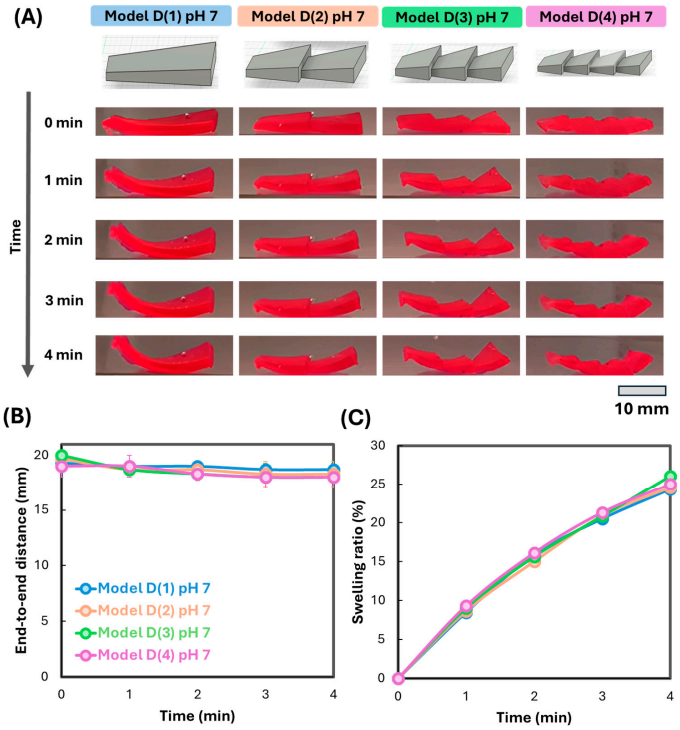


Figure 5. Hydrogel Actuators with Varying Numbers of Building Block Units at pH 7. (**A**) Curling behavior of the hydrogel during swelling over 4 min. (**B**) End-to-end distance of the curling hydrogel during swelling over 4 min. (**C**) Swelling ratio of the hydrogel during swelling over 4 min. Error bars indicate standard deviations.

3.3. Reversibility and Equilibrium of Hydrogel Soft Robotics

The actuation process of the hydrogels in this work is found to be reversible, depending on the water content within the hydrogel. This is demonstrated by the curling and uncurling of hydrogel actuators in Model D(4), as shown in Figure 6A,B. Initially, the hydrogel actuator is soaked in a pH 13 solution, causing the specimen to swell and curl within the first 4 min, as previously demonstrated in Section 3.2. Following this, the actuator is soaked in a volatile acetone to return to its original shape by removing water, resulting in uncurling over the next 4 min. This demonstrates the actuator's ability to curl and uncurl in response to changes in water content in the hydrogel. The process can be repeated, as shown in Figure 6A,B, which display two complete cycles of curling and uncurling in water and acetone, respectively. The reversibility of this actuator is due to the reduction of the swelling gradient within the specimens, allowing the hydrogel actuator to return to a form close to its original. This demonstrates the practical function of the developed hydrogels in applications where high and repeatable reversibility, such as in sensors, is essential.

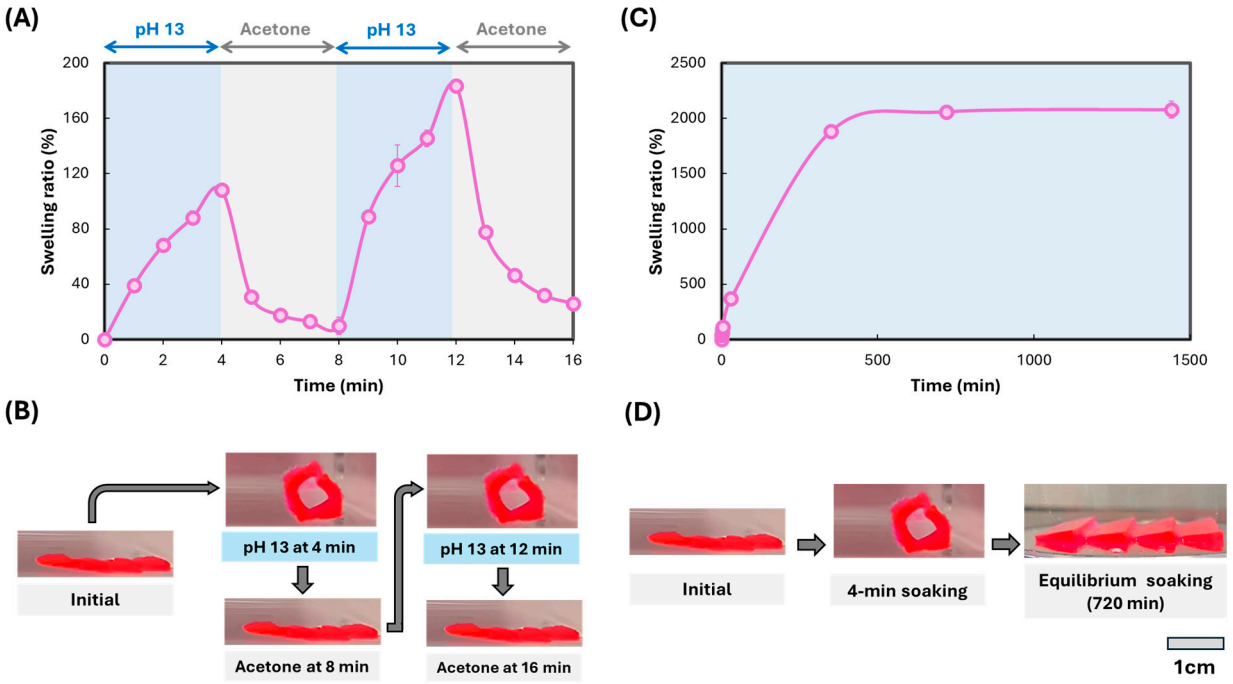


Figure 6. Reversibility and Equilibrium of the Model D(4) Hydrogel Actuators at pH 13. (**A**) Swelling ratio and swelling rate of the hydrogel actuator during alternating pH changes between pH 13 and acetone. (**B**) Digital illustration of the curling and uncurling of the hydrogel actuator during alternating pH changes between pH 13 and acetone. (**C**) Swelling ratio and swelling rate of the hydrogel actuator from initial to equilibrium swelling. (**D**) Digital illustration of the hydrogel actuator from initial to equilibrium swelling. Error bars indicate standard deviations.

Furthermore, the equilibrium of the hydrogel actuators is investigated in Figure 6C,D. It was found that the swelling of the hydrogel is rapid upon soaking in a pH 13 solution and slows down over time, flattening out at approximately 500 min. Regarding actuator response, the curling of the hydrogel actuator primarily occurs during the initial 4 min of curing for Model D(4) and maintains the curled state for about 20 min. Afterward, the hydrogel actuator gradually uncurls until it returns to its original shape. At equilibrium swelling, the actuator retains the same shape as the original but is significantly larger, characterized by a 2077% swelling ratio (Figure 6D). This indicates that the encoding building block design does not alter the equilibrium of the hydrogel but induces actuation during the initial swelling (or deswelling), where a significant gradient in water content exists within the specimen. Thus, the primary application of hydrogel actuators based on

this concept is in biomedical sensors, where fast, highly controllable, and precise actuation responses are crucial. Additionally, the mechanical properties of the equilibrium-swollen hydrogels were measured, showing a tensile strength of 0.29 MPa and a tensile strain of 180%, indicating significant softness compared to the as-printed state due to the substantial increase in water content.

3.4. Encoding Hydrogel Soft Robotics

Based on a series of hydrogel actuators developed using various building block designs and the assembled units described in Section 3.2, herein, we have demonstrated programmable encoding hydrogel soft robotics, as shown in Figure 7 and Video S2. A strip hydrogel robot is created by strategically arranging multiple hydrogel actuator units in specific orders and directions, resulting in more sophisticated actuator responses than a those of single actuator unit, enhancing versatility. In this case, each unit individually induces stress distribution within the structure through non-uniform swelling, governing the overall shape transformation. This concept is referred to as encoded hydrogel soft robotics, where the arrangement of each hydrogel actuator dictates the shape transformation of the entire structure. Such an integrated concept paves the way for further development of integrated uni-material designs.

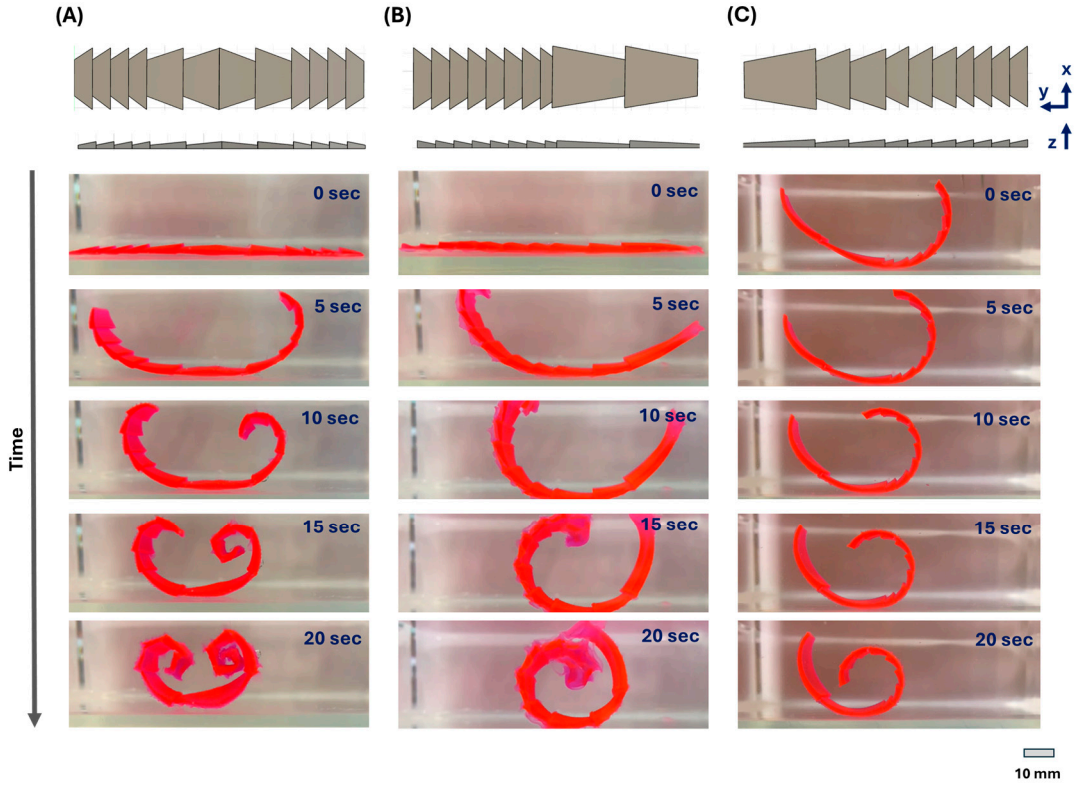


Figure 7. Shape Transformations of Encoded Hydrogel Soft Robotics at pH 13 and Their 3D Models. (**A**) Design code D4D2D4′D2′ for transforming into a heart shape. (**B**) Design code D1D1D4D4 for transforming into a spiral shape. (**C**) Design code D1D2D3D4 for transforming into a "6" shape. The video of the hydrogel shape transformation experiments shown in (**A**–**C**) can be found in Video S2 of the Supplementary Materials.

In Figure 7A, the transformation of a strip-shaped specimen into a heart shape is achieved by arranging four hydrogel actuators: Model D(4), Model D(2), and horizontally flipped versions of Model D(2) and Model D(4). This arrangement induces two levels of curling: a high degree of curling at the two ends based on Model D(4) and a lower degree of curling near the center based on Model D(2), forming a heart shape. The heart shape

forms because the stronger curling at the ends creates the rounded lobes, while the gentler curling in the center shapes the middle indentation. This design configuration, labeled as D4D2D4′D2′ in the code—with the apostrophe (′) indicating a laterally flipped model—allows for a more versatile actuation response. The approach enhances the potential for creating more complex hydrogel soft robotics using the 3D design concept.

Moreover, the code D1D1D4D4 creates a spiral shape by combining different curling intensities along the strip (Figure 7B). The D4 actuators on the left curl first with greater intensity due to their faster response, forming the initial tight spiral. The D1 actuators on the right then curl more gradually, extending the spiral shape as they follow. This sequence, with the stronger, quicker curl on the left and the gentler curl on the right, results in the formation of a spiral shape. Another example is the code D1D2D3D4 in Figure 7C, where varying degrees and speeds of curling are arranged from weakest (D1) to strongest (D4) from left to right. This generates a "6" shape, with the full curling effect on the right and a slight curling on the left. The results demonstrate the potential of this concept to create various complex actuation responses, primarily controlled by 3D design rather than material composition.

3.5. Potential Applications of Hydrogel Soft Robotics

Figure 8 demonstrates the application of encoded hydrogel soft robotics as a manipulator for transporting an object from one position to another. Two design codes are used: D4D4D4D4 for a fast-response manipulator and D2D2D2D2 for a slow-response manipulator (Figure 8 and Video S3). The hydrogel soft robotics are placed on a surface, and a pH-13 solution is poured to activate actuation, targeting the robotics to grasp the object and carry it to the designated goal. The D4D4D4D4 hydrogel quickly activates curling and transports the ball into the goal within 60 s, due to its high swelling gradient and rapid activation. In contrast, the D2D2D2D2 hydrogel begins curling only after 60 s, gradually grasps the object by around 120 s, and delivers it to the goal at about 150 s. This demonstration highlights the potential of encoding hydrogels for soft robotics applications that require precise and programmable actuation. The primary advantage of this approach over traditional methods is its simplicity: it uses a basic building block design with any type of hydrogel while providing high programmability through design. Modifying a hydrogel material can significantly alter its properties and introduce non-uniformities, making a design-focused approach more practical while leveraging existing materials. Systematic design and encoding enable these materials to function as efficient actuators across a range of applications, overcoming the limitations associated with complex material compositions.

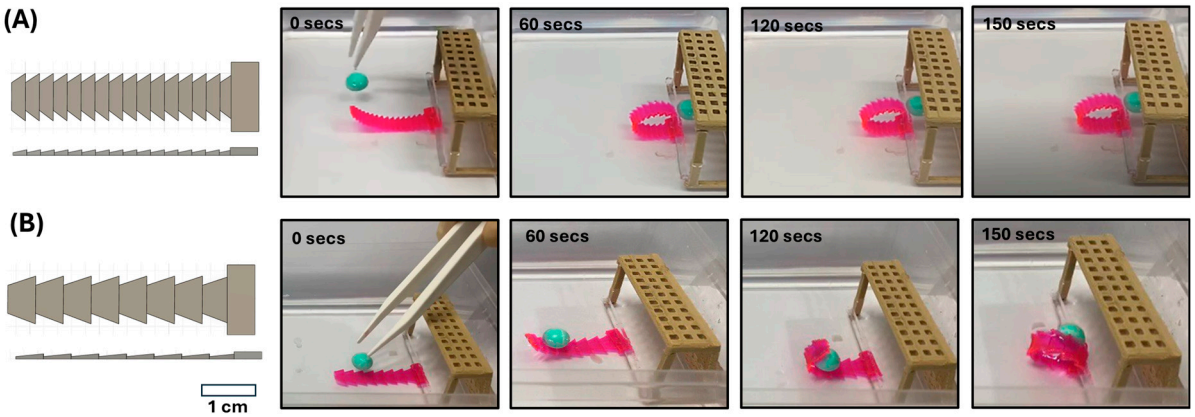


Figure 8. Application demonstration of hydrogel soft robotics as a manipulator, transporting an object from one position to another. (**A**) Design code D4D4D4D4 at pH 13, and (**B**) Design code D2D2D2D2 at pH 13. The video of the hydrogel soft robotics shown in (**A**,**B**) can be found in Video S3 of the Supplementary Materials.

The developed encoded hydrogel soft robotics hold significant promise in biomedical applications due to their biocompatibility and programmable kinetics. Compared to other materials, hydrogels hold significant potential in biomedical applications due to their high water content and ability to mimic biological tissues. Their actuation through immersion in a medium simulates the biological system's response to changes in water content, thereby enhancing their practical use in various biomedical applications. In contrast to methods that rely on external stimuli such as temperature or light, our soft robotics actuate through the intrinsic 3D structure of the hydrogel, utilizing swelling and deswelling in any aqueous medium. This independence from external stimuli enhances their practicality for real-world applications, making them more versatile and expanding their applicability across various biomedical settings compared to approaches that depend on variable stimuli conditions. The developed soft robotics are particularly promising as manipulators in minimally invasive surgeries and for targeted drug delivery, as similarly demonstrated in Figure 8. For example, these soft robotics can be utilized to deliver and deploy small medical devices or implants to precise locations within the body at specific times, ensuring accurate placement with minimal invasiveness [32–34]. Additionally, they can position surgical instruments with high precision, facilitating tasks such as cutting in confined spaces [35,36]. The actuation position and timing can be controlled by the design of different building block patterns and their assembly to achieve desired outcomes.

4. Conclusions

We have developed a generic approach for fabricating highly programmable hydrogel-based actuators using an encoded building block design concept. By maintaining uniform material properties, we achieved gradient swelling through the 3D design of material structures, enabling actuation upon immersion in a solution. Particularly focusing on a design perspective that ensures simple and versatile actuation, we employed various structural building block designs and different repeated building block units to create single-component hydrogel actuators with diverse actuation characteristics, including direction, degree, and kinetics of actuation. Key findings based on the encoded building block design concept include:

- The swelling gradient induced by the 3D structural design significantly influences actuation.
- Increasing the number of assembled actuation units results in a more pronounced actuation effect.
- Actuation is reversible throughout the swelling and shrinking processes.
- Actuation occurs primarily during the initial swelling or shrinking phase and diminishes as equilibrium is reached.
- The arrangement and sequencing of multiple actuation units can produce more complex and customizable responses.

This approach addresses the material design complexities and fabrication challenges typically associated with traditional property gradient-based hydrogel actuators by utilizing a single material and direct 3D printing. It streamlines the design strategy into a simple building block unit that can be applied across various scenarios to achieve hydrogel actuation, enabling straightforward adaptation to diverse applications through highly customizable encoding designs.

Supplementary Materials: The following supporting information can be downloaded at: https://www.mdpi.com/article/10.3390/act13100383/s1. Video S1: Hydrogel Actuators with Varying Numbers of Building Block Units. Video S2: Shape Transformations of Encoded Hydrogel Soft Robotics. Video S3: Application demonstration of hydrogel soft robotics as a manipulator.

Author Contributions: F.W., Z.A.C. and S.P. conceived the idea, developed the outline, designed the experiment; Z.A.C. and Y.T.C. prepared samples and performed the experimental measurements; S.P. and F.W. supported the experiments. S.P., Z.A.C. and F.W. analyzed the data and wrote the

manuscript with contributions from all authors. All authors have read and agreed to the published version of the manuscript.

Funding: The authors acknowledge the financial support from A*STAR under the RIE2025 Manufacturing, Trade and Connectivity (MTC) Programmatic Fund. Grant No: M24N3b0028. This work was also financially supported by the A*STAR Career Development Fund (Grant No: C233312015).

Data Availability Statement: The data presented in this study are available on request from the corresponding author.

Acknowledgments: We extend our gratitude to Hannah Lim of IMRE and Yu Hong Cheang of Nanyang Polytechnic for their invaluable experimental and laboratory support. We also appreciate the insightful suggestions provided by Zehuang Lin and Rigel Lu Jun Teo of NUS during our experiments.

Conflicts of Interest: The authors declare no conflict of interest.

References

1. Chen, Y.; Zhang, Y.; Li, H.; Shen, J.; Zhang, F.; He, J.; Lin, J.; Wang, B.; Niu, S.; Han, Z.; et al. Bioinspired Hydrogel Actuator for Soft Robotics: Opportunity and Challenges. *Nano Today* **2023**, *49*, 101764. [CrossRef]
2. Cheng, F.-m.; Chen, H.-x.; Li, H.-d. Recent Progress on Hydrogel Actuators. *J. Mater. Chem. B* **2021**, *9*, 1762–1780. [CrossRef] [PubMed]
3. Lee, Y.; Song, W.J.; Sun, J.Y. Hydrogel Soft Robotics. *Mater. Today Phys.* **2020**, *15*, 100258. [CrossRef]
4. López-Díaz, A.; Vázquez, A.S.; Vázquez, E. Hydrogels in Soft Robotics: Past, Present, and Future. *ACS Nano* **2024**, *18*, 20817–20826. [CrossRef]
5. Jiang, J.; Xu, S.; Ma, H.; Li, C.; Huang, Z. Photoresponsive Hydrogel-Based Soft Robot: A Review. *Mater. Today Bio* **2023**, *20*, 100657. [CrossRef]
6. Park, C.S.; Kang, Y.-W.; Na, H.; Sun, J.-Y. Hydrogels for Bioinspired Soft Robots. *Prog. Polym. Sci.* **2024**, *150*, 101791. [CrossRef]
7. Deligkaris, K.; Tadele, T.S.; Olthuis, W.; van den Berg, A. Hydrogel-Based Devices for Biomedical Applications. *Sens. Actuators B Chem.* **2010**, *147*, 765–774. [CrossRef]
8. Hoffman, A.S. Hydrogels for Biomedical Applications. *Adv. Drug Deliv. Rev.* **2012**, *64*, 18–23. [CrossRef]
9. Sánchez-Cid, P.; Jiménez-Rosado, M.; Romero, A.; Pérez-Puyana, V. Novel Trends in Hydrogel Development for Biomedical Applications: A Review. *Polymers* **2022**, *14*, 3023. [CrossRef]
10. Pruksawan, S.; Chee, H.L.; Wang, Z.; Lee, Y.L.; Sivaraja, V.K.S.O.; Ow, S.Y.; Li, J.; Wang, F. Gold Nanorods Function as near-Infrared Light-Activated Microheaters for in Situ Curing of Injectable Hydrogel Therapies. *ACS Appl. Polym. Mater.* **2023**, *5*, 4565–4577. [CrossRef]
11. Odent, J.; Vanderstappen, S.; Toncheva, A.; Pichon, E.; Wallin, T.J.; Wang, K.; Shepherd, R.F.; Dubois, P.; Raquez, J.-M. Hierarchical Chemomechanical Encoding of Multi-Responsive Hydrogel Actuators Via 3d Printing. *J. Mater. Chem. A* **2019**, *7*, 15395–15403. [CrossRef]
12. Nishiguchi, A.; Zhang, H.; Schweizerhof, S.; Schulte, M.F.; Mourran, A.; Möller, M. 4D Printing of a Light-Driven Soft Actuator with Programmed Printing Density. *ACS Appl. Mater. Interfaces* **2020**, *12*, 12176–12185. [CrossRef] [PubMed]
13. Simińska-Stanny, J.; Nizioł, M.; Szymczyk-Ziółkowska, P.; Brożyna, M.; Junka, A.; Shavandi, A.; Podstawczyk, D. 4D Printing of Patterned Multimaterial Magnetic Hydrogel Actuators. *Addit. Manuf.* **2022**, *49*, 102506. [CrossRef]
14. Li, Y.; Zheng, W.; Li, B.; Dong, J.; Gao, G.; Jiang, Z. Double-Layer Temperature-Sensitive Hydrogel Fabricated by 4D Printing with Fast Shape Deformation. *Colloids Surf. A Physicochem. Eng. Asp.* **2022**, *648*, 129307. [CrossRef]
15. Tang, L.; Wu, X.; Xu, Y.; Li, Y.; Wu, S.; Gong, L.; Tang, J. Bilayer Hydrogel Actuators with High Mechanical Properties and Programmable Actuation Via the Synergy of Double-Network and Synchronized Ultraviolet Polymerization Strategies. *Polymers* **2024**, *16*, 840. [CrossRef]
16. Mo, K.; He, M.; Cao, X.; Chang, C. Direct Current Electric Field Induced Gradient Hydrogel Actuators with Rapid Thermo-Responsive Performance as Soft Manipulators. *J. Mater. Chem. C* **2020**, *8*, 2756–2763. [CrossRef]
17. Chen, Y.; Chen, Z.; Chen, C.; Ur Rehman, H.; Liu, H.; Li, H.; Hedenqvist, M.S. A Gradient-Distributed Liquid-Metal Hydrogel Capable of Tunable Actuation. *Chem. Eng. J.* **2021**, *421*, 127762. [CrossRef]
18. Pruksawan, S.; Lin, Z.; Lee, Y.L.; Chee, H.L.; Wang, F. 4D-Printed Hydrogel Actuators through Diffusion-Path Architecture Design. *ACS Appl. Mater. Interfaces* **2023**, *15*, 46388–46399. [CrossRef]
19. Kameoka, M.; Watanabe, Y.; Shiblee, M.N.; Kawakami, M.; Ogawa, J.; Khosla, A.; Furukawa, H.; Zhang, S.; Hirai, S.; Wang, Z. 4D Printing of Hydrogels Controlled by Hinge Structure and Spatially Gradient Swelling for Soft Robots. *Machines* **2023**, *11*, 103. [CrossRef]
20. Pruksawan, S.; Lim, J.W.R.; Lee, Y.L.; Lin, Z.; Chee, H.L.; Chong, Y.T.; Chi, H.; Wang, F. Enhancing Hydrogel Toughness by Uniform Cross-Linking Using Modified Polyhedral Oligomeric Silsesquioxane. *Commun. Mater.* **2023**, *4*, 75. [CrossRef]
21. Pruksawan, S.; Chee, H.L.; Wang, Z.; Luo, P.; Chong, Y.T.; Thitsartarn, W.; Wang, F. Toughened Hydrogels for 3D Printing of Soft Auxetic Structures. *Chem.–Asian J.* **2022**, *17*, e202200677. [CrossRef]

22. Gerlach, G.; Guenther, M.; Sorber, J.; Suchaneck, G.; Arndt, K.-F.; Richter, A. Chemical and Ph Sensors Based on the Swelling Behavior of Hydrogels. *Sens. Actuators B Chem.* **2005**, *111–112*, 555–561. [CrossRef]
23. Peng, X.; Wang, H. Shape Changing Hydrogels and Their Applications as Soft Actuators. *J. Polym. Sci. Part B Polym. Phys.* **2018**, *56*, 1314–1324. [CrossRef]
24. Myagchenkov, V.A.; Kurenkov, V.F. Applications of Acrylamide Polymers and Copolymers: A Review. *Polym.-Plast. Technol. Eng.* **1991**, *30*, 109–135. [CrossRef]
25. Sennakesavan, G.; Mostakhdemin, M.; Dkhar, L.K.; Seyfoddin, A.; Fatihhi, S.J. Acrylic Acid/Acrylamide Based Hydrogels and Its Properties—A Review. *Polym. Degrad. Stab.* **2020**, *180*, 109308. [CrossRef]
26. Faturechi, R.; Karimi, A.; Hashemi, A.; Yousefi, H.; Navidbakhsh, M. Influence of Poly(Acrylic Acid) on the Mechanical Properties of Composite Hydrogels. *Adv. Polym. Technol.* **2015**, *34*, 21487. [CrossRef]
27. Gupta, P.; Vermani, K.; Garg, S. Hydrogels: From Controlled Release to Ph-Responsive Drug Delivery. *Drug Discov. Today* **2002**, *7*, 569–579. [CrossRef]
28. Turan, E.; Çaykara, T. Swelling and Network Parameters of pH-Sensitive Poly(Acrylamide-Co-Acrylic Acid) Hydrogels. *J. Appl. Polym. Sci.* **2007**, *106*, 2000–2007. [CrossRef]
29. Rizwan, M.; Yahya, R.; Hassan, A.; Yar, M.; Azzahari, A.D.; Selvanathan, V.; Sonsudin, F.; Abouloula, C.N. pH Sensitive Hydrogels in Drug Delivery: Brief History, Properties, Swelling, and Release Mechanism, Material Selection and Applications. *Polymers* **2017**, *9*, 137. [CrossRef]
30. Andrade, F.; Roca-Melendres, M.M.; Durán-Lara, E.F.; Rafael, D.; Schwartz, S. Stimuli-Responsive Hydrogels for Cancer Treatment: The Role of pH, Light, Ionic Strength and Magnetic Field. *Cancers* **2021**, *13*, 1164. [CrossRef]
31. Willner, I. Stimuli-Controlled Hydrogels and Their Applications. *Acc. Chem. Res.* **2017**, *50*, 657–658. [CrossRef] [PubMed]
32. Dou, W.; Zhong, G.; Cao, J.; Shi, Z.; Peng, B.; Jiang, L. Soft Robotic Manipulators: Designs, Actuation, Stiffness Tuning, and Sensing. *Adv. Mater. Technol.* **2021**, *6*, 2100018. [CrossRef]
33. Chen, X.; Zhang, X.; Huang, Y.; Cao, L.; Liu, J. A Review of Soft Manipulator Research, Applications, and Opportunities. *J. Field Robot.* **2022**, *39*, 281–311. [CrossRef]
34. Ghosh, A.; Yoon, C.; Ongaro, F.; Scheggi, S.; Selaru, F.M.; Misra, S.; Gracias, D.H. Stimuli-Responsive Soft Untethered Grippers for Drug Delivery and Robotic Surgery. *Front. Mech. Eng.* **2017**, *3*, 00007. [CrossRef] [PubMed]
35. Zhu, J.; Lyu, L.; Xu, Y.; Liang, H.; Zhang, X.; Ding, H.; Wu, Z. Intelligent Soft Surgical Robots for Next-Generation Minimally Invasive Surgery. *Adv. Intell. Syst.* **2021**, *3*, 2100011. [CrossRef]
36. Mendez, K.; Whyte, W.; Freedman, B.R.; Fan, Y.; Varela, C.E.; Singh, M.; Cintron-Cruz, J.C.; Rothenbücher, S.E.; Li, J.; Mooney, D.J.; et al. Mechanoresponsive Drug Release from a Flexible, Tissue-Adherent, Hybrid Hydrogel Actuator. *Adv. Mater.* **2023**, 2303301. [CrossRef]

Disclaimer/Publisher's Note: The statements, opinions and data contained in all publications are solely those of the individual author(s) and contributor(s) and not of MDPI and/or the editor(s). MDPI and/or the editor(s) disclaim responsibility for any injury to people or property resulting from any ideas, methods, instructions or products referred to in the content.